Order-of-magnitude increase in flow velocity driven by mass conservation during the evaporation of sessile drops

Order-of-magnitude increase in flow velocity driven by mass conservation during the evaporation of sessile drops

Yoshinori Hamamoto,[1,2] John R. E. Christy,[1] and Khellil Sefiane[1,*]
[1]*School of Engineering, The University of Edinburgh, Kings Buildings, Edinburgh EH9 3JL, United Kingdom*
[2]*Department of Mechanical Engineering, Kyushu University, Fukuoka 819-0395, Japan*
(Received 12 November 2010; revised manuscript received 11 January 2011; published 3 May 2011)

We report on a dramatic order-of-magnitude increase in flow velocity within pinned evaporating droplets toward the end of their lifetime. The measurements were performed using high-speed microparticle image velocimetry. The study revealed interesting observations about the spatial and temporal evolution of the velocity field. The profile along the radius of the droplet is found to exhibit a maximum toward the three phase contact line with flow oscillations in time in this region. Additional optical measurements allowed further analysis of the observed trends. Analysis of the potential mechanisms responsible for the flow within the droplet demonstrated that these observations can be satisfactorily explained and accounted for by mass conservation within the droplet to compensate for evaporation.

DOI: 10.1103/PhysRevE.83.051602 PACS number(s): 68.08.Bc, 68.03.Fg

I. INTRODUCTION

Droplet evaporation has attracted much interest recently, being a fundamental process relevant to a wide range of biological and technological applications. While physicists are still largely discussing issues of wettability and spreading of drops, in Bonn *et al*.'s review of the subject [1], they describe the area of evaporating droplets as being a hot topic for further investigation. The underlying mechanisms for this seemingly simple phenomenon are still being debated among researchers with many aspects still poorly understood. Recently, Ghasemi and Ward [2] have demonstrated that convection within evaporating droplets plays a major role in energy transport during the evaporation process. The authors found that thermocapillary convection, for water droplets evaporating in a reduced pressure environment, is by far the largest mode of energy transport along the surface of the drop, accounting for around 95% of the energy transfer. This is in stark contrast to earlier studies [3] for heated drops. The authors have also reported a Marangoni driven flow adjacent to the liquid-vapor interface from the edge of the drop toward the apex.

Shahidzadeh-Bonn *et al*. [4] have shown that for evaporating water drops on a smooth surface, where contact line pinning does not occur, the radius shrinks in proportion to $(t_f - t)^{0.6}$, whereas for organic liquids, such as hexane, the radius shrinks as $(t_f - t)^{0.5}$. They attribute this difference to convection in the vapor induced by water vapor being lighter than air and demonstrate this by enclosing a water drop so that circulation of the air due to rising water vapor is not possible and by using forced convection for a hexane drop. The exponents found in these revised experiments for radius versus time remaining were 0.5 and 0.6, respectively (i.e., the reverse of the original experiments), indicating that induced convection in the vapor can explain the difference in evaporation dynamics.

The original work of Deegan *et al*. [5] showed ring stain formation as a direct result of evaporation of suspension-containing droplets. Deegan *et al*. [5,6] observed outward motion in pinned drops by seeding the drop with solid particles. Deegan *et al*. explained the flow in terms of mass conservation. Ring formation at the periphery of the drop, resulting from the deposition of the solid particles was attributed to the strong evaporation from the edge. Based solely on mass conservation, a very simple theoretical description of the flow inside the drop was given. The flow in the vapor was assumed diffusion limited. The boundary condition for the rate of mass loss per unit surface area per unit time was derived by analogy with the electric field divergence near a sharp edge on a charged conductor. The calculated values of the mass flux at the surface as a function of the distance from the center of the drop increase by two orders of magnitude from the center to the edge. This edge enhancement of flux is attributed to the greater probability of an evaporating molecule's escape when departing from the edge than when leaving from the apex of the drop. Deegan *et al*. [5], on the basis of their theory, suggest that for small contact angles the velocity varies with time, t, as $(t_f - t)^{-1}$, where t_f is the lifespan of the drop, and with radius, r, in the region close to the contact line as $(R - r)^{-\lambda}$, where $\lambda = (\pi - 2\theta_c)/(2\pi - 2\theta_c)$ and θ_c is the contact angle. For small contact angles, $\lambda \approx 1/2$. They report that they measured the velocities by particle tracking but have not provided the full spatial and temporal velocity maps in their paper. Since those earlier papers [5,6] on the evaporation of pinned sessile drops, several attempts have been made to rationalize various experimental results.

On the other hand, Marangoni flow, as reported in Ref. [2], is driven by local cooling that varies in magnitude following the intensity of evaporation. Surface tension gradients thus generated on the liquid-gas interface lead to thermocapillary flow as observed by Buffone *et al*. [7] in the case of a meniscus evaporating in a capillary and by Ghasemi and Ward in sessile drops [2].

Over the years many experimental and theoretical studies have been devoted to understanding the dynamics of droplet evaporation, including its internal flow. This latter can not only influence the evaporation kinetics but also affect the ring deposits. The theoretical investigation of Hu and Larson [8]

*Corresponding author: ksefiane@ed.ac.uk

has shown that there is a thermocapillary driven flow within the droplet that can change as the droplet profile evolves. The work of Ristenpart *et al*. [9] has shown that the relative thermal properties of the substrate and the liquid can affect the direction of flow within evaporating droplets. Xu *et al*. [10] revealed, using fluorescent particles as tracers, that there is Marangoni flow in evaporating water droplets, with a stagnation point at the droplet surface, where the surface flow, the surface tension gradient, and the surface temperature gradient change their directions.

Xu *et al*. [11] have shown that the direction of the flow depends on the contact angle, with the direction reversing at a critical contact angle, which depends not only on the relative thermal conductivities of the substrate and liquid but also on the ratio of the substrate thickness to the contact-line radius of the droplet. Experimental data indicate a linear dependency of the overall evaporative mass flux with the wetting radius. This has been used as an argument to point to the conclusion that most of evaporation is concentrated near the contact line. Numerical calculations have been carried out on basis of a first model developed by Hu and Larson [12] that took as a starting point for evaporation the diffusion process in the vapor. The results of the model of Hu and Larson [8] shows that the Marangoni flow runs from the contact line to the apex of the drop, adjacent to the liquid-vapor interface. They also show that there is a return flow at the bottom of the drop from the center to the edge of the drop. The exact nature and evolution of flow within evaporating droplets is not fully elucidated. The contribution of this latter to energy transport is another important outstanding issue [2]. Other investigations have demonstrated using mathematical and numerical modeling similar flow for heated droplets [13,14], where the dynamics differ substantially from those encountered here.

In order to address the outstanding issues about the nature and evolution of flow within evaporating droplets, experimental particle image velocimetry (PIV) analysis of the full flow field and its evolution in time is required. There is clearly a need for further experimental work on flow field within evaporating droplets and its evolution in time.

II. EXPERIMENTAL METHOD

Microparticle image velocimetry (μPIV) was used to obtain velocity information within evaporating sessile drops. Droplets of distilled water [0.12 μl ($\pm$0.03 μl)], seeded with 0.04% solids of fluorescent microspheres (1-μm diameter, Nile red, carboxylate modified FluoSphere beads of density 1.05 g/cm^3), were injected onto a clean glass cover slide, sitting on an inverted microscope (Leica DM15000 M) to yield sessile drops with a diameter of about 1 mm. Due to the presence of seeding particles, the drops are self-pinning on the glass substrate. A New Wave Pegasus pulse diode laser emitting at 527 nm, synchronized with a Dantec Dynamics Nanosense II camera (512 $\times$ 512 pixels, spatial resolution 512 pixels/1.6 mm) at 10 Hz, was used to cause the particles to fluoresce at 575 nm and the resulting images were captured. Velocities of the particles in the horizontal plane were determined by cross-correlation of successive images. The height, above the base of the drop, of the plane in which the velocities were determined was set by adjusting the focus on the microscope. Measurements of the velocity distribution were taken in three horizontal planes above the glass cover slide. The focal plane was centered on three horizontal positions; just above (1 μm) the cover slide, 30 μm above, and 60 μm above. Note that the relative heights off the base are more important here than the absolute values, since the microscope has a depth of field of around 20–30 μm. The images were recorded at a resolution of 320 pixels/mm. The drop profile was also captured by charge-coupled device camera for the same size of pure water droplets evaporated on glass cover slides and the evolution in time of the contact angle, base width, height, and volume were determined using a Kruss DSA 100 drop shape analysis system.

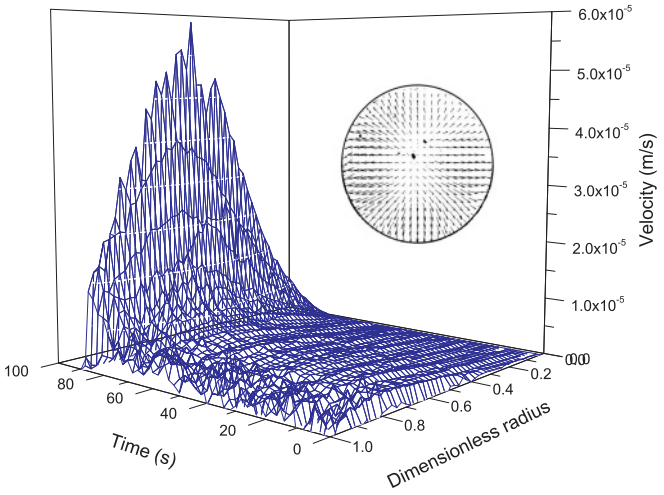

FIG. 1. (Color online) Three-dimensional Spatiotemporal evolution of the flow field, measured just above the base of the drop (within 30 μm), in an evaporating water droplet. Inset shows that the velocity vectors are those of a radially outward flow.

III. RESULTS AND DISCUSSION

μPIV measurements close to the base of a sessile water drop on a glass substrate reveal a symmetrical horizontal flow component radially outward (see vector map inset in Fig. 1) which increases from zero at the center to a maximum at about 70% of the radius of the drop. The velocity values in Fig. 1 are averages around the drop for each radial position. As expected, the drop remains pinned throughout, due to the presence of deposited particles at the contact line, and the evaporation rate remains constant [Fig 2(a)].

As evaporation proceeds, two effects are observed (Fig. 1): The radial velocity at each radial position increases, rising dramatically toward the end of the lifetime of the drop, and temporal oscillations are observed in the radial velocities near the outer edge of the drop. Figure 3 shows the velocity plotted against time for $r/R_{\mathrm{ini}} = 0.1$ and 0.9, demonstrating more clearly the order of magnitude velocity rise and the temporal oscillation in velocity near the edge of the drop. Note that there is an order of magnitude difference between the velocity of the liquid near the outer edge of the drop (90% of radius) and that close to the center (10% of radius) and, toward the end of the lifespan of the drop, there is an order of magnitude increase in the velocity relative to that in the early stages of evaporation.

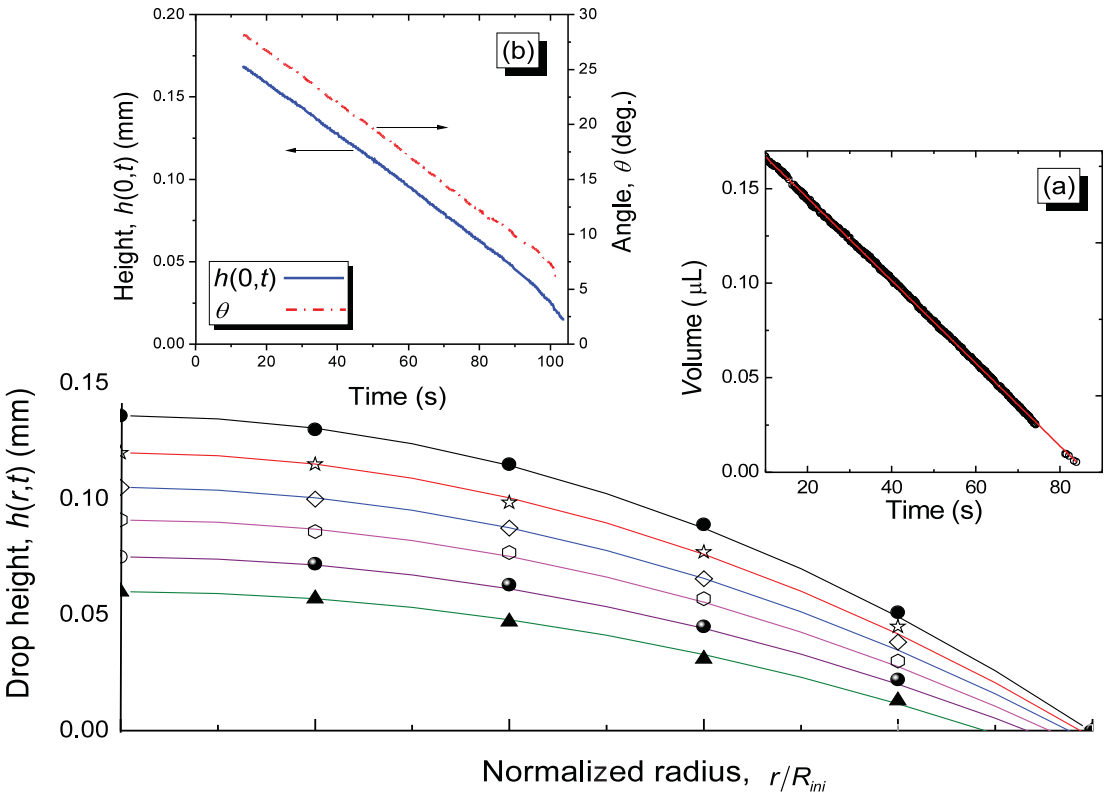

FIG. 2. (Color online) Profile of evaporating water droplet on a glass slide from optical measurements (DSA 100). (a) Linear evolution of volume in time, indicating constant evaporation rate; (b) contact angle (in the range of 30°–5°) and height in time.

The increase in velocity toward the end of the lifetime of the drop can be explained on the basis of mass conservation. The evaporation rate was constant at about 0.0014 μl/s throughout, while the height of droplet decreases with time [Fig 2(b)]. It is known that evaporation occurs preferentially near the contact line, so with a reduced cross-sectional area for flow due to the drop height decreasing with time, and a constant volumetric flow to the contact line, to match the evaporation here, the velocity at any radial position must increase as the evaporation proceeds. Also plotted on Fig. 3 is the best fit line for velocity versus $A(t_f - t)^{-1}$, the anticipated temporal variation predicted by Deegan *et al.* [5,6].

It can be seen that there is good agreement between Deegan's prediction and our results. The vertically averaged radial flow velocity, $v_r(r,t)$, was estimated, using our measured evaporation rate, by considering mass conservation of fluid for one-dimensional radial flow in the droplet at a quasi-steady state.

$$v_r(r,t) = \left[-dV/dt - \int_0^r J(r,t)dS(r,t)\right] \Big/ 2\pi r h(r,h),$$

where $J(r,t)$ and $S(r,t)$ denote the local mass flux by evaporation and interface surface area, respectively. This equation does not consider Marangoni flow on the surface of the droplet. The total evaporation rate, dV/dt, and the local droplet height, $h(r,t)$, were input from the optical measurements data. We considered two cases: In the first, $J = 0$, as would be the case for evaporation occurring only at the contact line; in the second we assumed uniform evaporation over the whole surface (i.e., J constant). Figure 4 shows the comparison of estimated velocity with measurements at $r/R_{\text{ini}} = 0.7$ for both cases.

In the first case, the shape of the velocity profile with time matches the μPIV measurements, but the measured velocity is lower than that predicted. In the second case, the velocity profile does not show the same dramatic rise, but the velocities in the early stage of evaporation are close to those measured using PIV. The maximum radial velocity v_{rmax} was 4.5 $\times$ 10^{-5} m/s $\pm$1.3 $\times$ 10^{-5} m/s. That the former

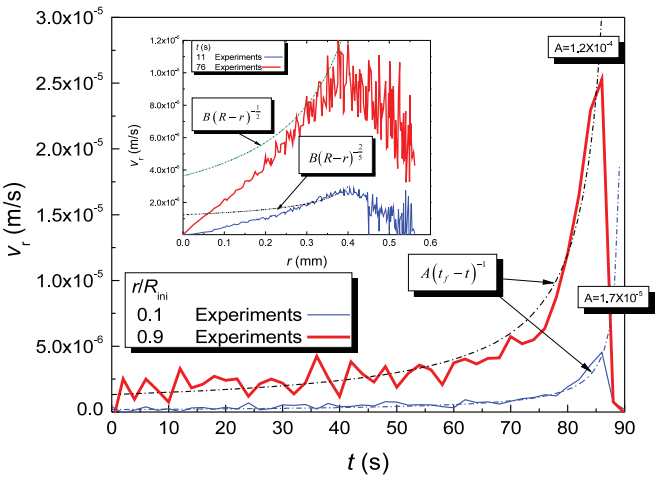

FIG. 3. (Color online) Comparisons of averaged radial flow velocity $v_r(r, t)$ at two radial positions. Inset shows profile of velocity as a function of radial position.

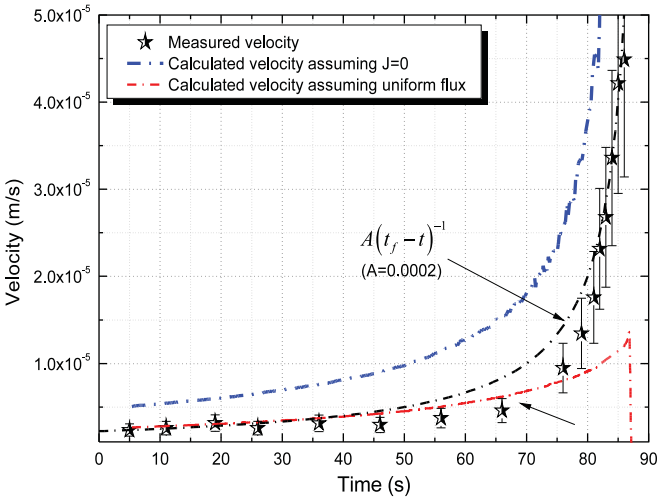

FIG. 4. (Color online) Comparison of velocity evolution in time between measured data and predictions made on the basis of mass conservation alone.

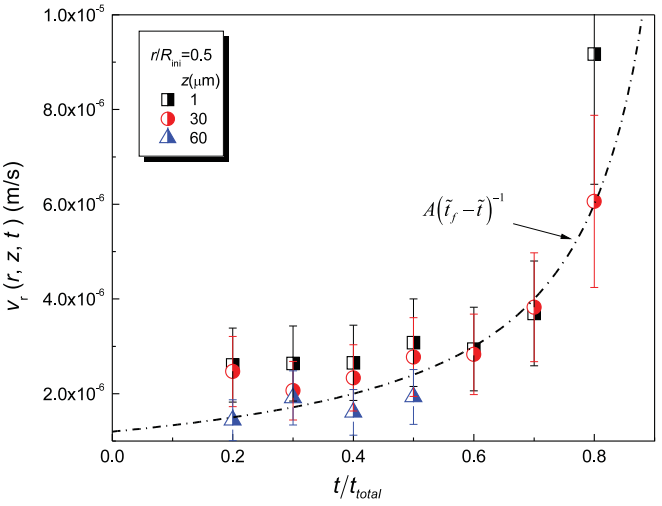

FIG. 5. (Color online) Comparison of velocity at various depths from the substrate surface.

case should overpredict the velocity can be explained by not all the evaporation occurring at the contact line, so $J \neq 0$. This is in agreement with the work of Shahidzadeh-Bonn *et al*. [4], who indicate that induced convection in the vapor leads to enhanced evaporation from the drop surface. However, as the contact angle decreases, the proportion of evaporation occurring at the contact line increases, so $J = 0$ becomes a good approximation in the latter stages of evaporation. This suggests that the flow in the droplet is mainly governed by simple mass conservation around $r/R_{\text{ini}} = 0.7$, with evaporation largely occurring close to the contact line. We have plotted a best fit line of $v = A(t_f - t)^{-1}$ in Fig. 4, which shows reasonable agreement with the variation of the experimental data. It should be noted that the value of A here has not been predicted from first principles, so we cannot comment on the relative magnitude of the experimental velocity values and those on the best fit line. In comparing the variation of radial velocity with radius with that predicted by Deegan (inset of Fig. 3), it is clear that, even at the contact line, where Deegan's prediction of velocity varying as $(R - r)^{-}\lambda$ ought to apply, there is no agreement with our experimental data. In our experiments, λ ranges from about $2/5$ early in the evaporation (blue experimental line) to $\frac{1}{2}$ late in the evaporation (red experimental curve) as the contact angle decreases from about $\pi/6$ to zero. Our measured velocities vary from zero, as expected, at the center of the drop to a maximum at about 70% of the drop radius. Mass conservation with the majority of evaporation at the contact line would result in the velocity continuing to increase right up to the contact line, as predicted by Deegan's formula. That the velocity decreases in the last 20–30% of the radius toward the contact line is an indication that enhanced evaporation is not limited to the contact line itself and may indeed be occurring over a region close to the contact line. Since this deviation in behavior is most significant in the outer 30% of the radius of the drop, it is reasonable to assume that enhanced evaporation occurs over all of this outer region. At the end of evaporation a circular deposition pattern is found, indicating that the seeding particles had deposited preferentially at the contact line. This is consistent with the majority of the evaporation occurring near the contact line and with evaporation being limited to the contact line during the latter stages of dryout of the drop.

Our work therefore supports the prediction of Deegan *et al*. [6] that the flow within the droplet arises from mass conservation, since Marangoni convection from the contact line to the apex would lead to higher velocities along the base of the drop than those required to satisfy mass conservation due to evaporation. At first sight it contradicts the results of Ghasemi and Ward [2]. However, it is important that the relative importance of the Marangoni effect is evaluated for our experiments. It is worth noting that the experimental results in Ref. [2] are for an enhanced evaporation rate in a reduced-pressure environment. This might point to the fact that Marangoni flow contribution becomes a more significant energy transport mechanism as evaporation rate increases. In these experiments, the contact angle varied between about 30° and 5°, as shown in Fig. 2. Under these conditions, the influence of Marangoni flow may be assumed to be negligible, as the variation in drop height with radius and hence thermal conduction from the solid substrate to the surface of the drop is small. Indeed, infrared measurements suggest less than 0.3 K of a temperature difference between the contact line and the apex of the drop. As the drop evaporates the conduction length decreases, so variations in temperature along the interface must also decrease. If the flow were influenced by Marangoni convection, we would therefore expect the velocities measured to decrease with time. The fact that the velocity increases is therefore supporting evidence for mass conservation being the driving force for the measured velocities in this study.

Figure 5 shows the velocity distribution in each plane over the evaporation lifetime. There is no significant difference in velocity with distance from the cover slide, suggesting a uniform flow distribution in the vertical direction at each radial position. This is in agreement with the velocity profiles predicted by Hu and Larson [12] for low contact angles, where Marangoni convection has little influence. Indeed, the order of magnitude of the velocities predicted by Hu and Larson (10^{-5} m/s) is in agreement with those measured in our study.

It is possible that with substrates having different thermal and wetting properties to glass or with evaporation of fluids with different thermal or wetting characteristics, the flow could indeed be influenced by Marangoni convection in which case we would expect higher measured velocities outward near the base of the drop and reduction of these outer velocities with height due to recirculation within the drop set up by Marangoni convection [15]. For water, previous studies have shown limited influence of Marangoni convection. Indeed previous work in our laboratory on the meniscus in a capillary revealed no Marangoni convection with water but significant Marangoni convection with alcohols [7]. The present results are consistent and in agreement with previous investigations on the evaporation of liquids in capillary tubes, Ref. [16].

In conclusion, the velocity profile along the radius of the droplet is found to exhibit a maximum toward the three-phase contact line. The evolution in time shows a dramatic increase in the velocity toward the end of the droplet lifetime. Using optical measurements in conjunction with μPIV allowed further analysis of the observed trends. An analysis of the potential mechanisms responsible for the flow within the droplet demonstrated that these observations can be accounted for by mass conservation alone.

[1] D. Bonn, J. Eggers, J. Indekeu, J. Meunier, and E. Rolley, Rev. Mod. Phys. **81**, 739 (2009).

[2] H. Ghasemi and C. A. Ward, Phys. Rev. Lett. **105**, 136102 (2010).

[3] F. Girard, M. Antoni, and K. Sefiane, Langmuir **24**, 9207 (2008).

[4] N. Shahidzadeh-Bonn, S. Rafai, A. Azouni, and D. Bonn, J. Fluid Mech. **549**, 307 (2006).

[5] R. D. Deegan, O. Bakajin, T. F. Dupont, G. Huber, S. R. Nagel, and T. A. Witten, Nature **389**, 827 (1997).

[6] R. D. Deegan, O. Bakajin, T. F. Dupont, G. Huber, S. R. Nagel, and T. A. Witten, Phys. Rev. E **62**, 756 (2000).

[7] C. Buffone, K. Sefiane, and J. Christy, Phys. Fluids **17**, 052104 (2005).

[8] H. Hu and R. G. Larson, Langmuir **21**, 3972 (2005).

[9] W. D. Ristenpart, P. G. Kim, C. Domingues, J. Wan, and H. A. Stone, Phys. Rev. Lett. **99**, 234502 (2007).

[10] X. F. Xu and J. B. Luo, Appl. Phys. Lett. **91**, 124102 (2007).

[11] Xu Xuefeng, Luo Jianbin, and Guo Dan, Langmuir **26**, 1918 (2010).

[12] H. Hu and R. G. Larson, J. Phys. Chem B **110**, 7090 (2006).

[13] G. J. Dunn, S. K. Wilson, B. R. Duffy, S. David, and K. Sefiane, Colloid. Surface. A **323**, 50 (2008).

[14] F. Duan, J. Phys. D: Appl. Phys **42**, 102004 (2009).

[15] G. J. Dunn, S. K. Wilson, B. R. Duffy, S. David, and K. Sefiane, J. Fluid Mech. **623**, 329 (2009).

[16] C. Buffone, K. Sefiane, and W.J. Easson, Phys. Rev. E **71**, 056302 (2005).